RSC Advances

COMMUNICATION

View Article Online
View Journal | View Issue

Cite this: *RSC Adv.*, 2016, **6**, 1644

Received 15th November 2015
Accepted 17th December 2015

DOI: 10.1039/c5ra24133b

www.rsc.org/advances

The fluorescence detection of autophagosomes in live cells under starvation using core-substituted naphthalenediimide probes†

Namdev V. Ghule,[a] Kiran Kharat,*[b] Rajesh S. Bhosale,[a] Avinash L. Puyad,[c] Sheshanath V. Bhosale*[d] and Sidhanath V. Bhosale*[a]

A naphthalenediimide colorimetric pH sensor was designed, synthesised and employed for live cell applications. In DMSO : buffer solution, the NDI probe exhibits good pH selectivity and high photostability. We used a core-substituted naphthalenediimide (**NDI-C**) probe for the analysis of the autophagosomes. A new flow cytometric method was also developed for the analysis of cell population on the basis of intracellular pH.

Eukaryotic cells employ autophagy to degrade damaged or obsolete organelles and proteins. Central to this process is the formation of autophagosomes, double-membrane vesicles responsible for delivering cytoplasmic material to lysosomes.[1] Autophagy is a system for degradation of bulk cellular components in lytic compartments, vacuoles, or lysosomes when eukaryotic cells are faced with nutrient starvation. Autophagic cell death is characterized by the sequestration of cytoplasm and organelles in double or multimembrane vesicles and delivery to the cells' own lysosomes for subsequent degradation.[2,3] In a sense, the cell "cannibalizes" itself. The mechanisms and morphology of autophagy are evolutionarily conserved with strong similarities between organisms as diverse as animals, plants and yeast.

The outer membranes of the autophagosomes ultimately fuse with the vacuole and the cellular components enclosed by the inner membranes are released into the vacuolar lumen as autophagic bodies. Finally, the autophagic bodies are disintegrated and their contents are degraded by vacuolar hydrolases.[4]

pH-Sensitive fluorescent probes are widely used in the analysis of the pH of the cells and organelles (Table S1; ESI†). 2,7-Bis-carboxyethyl-5,6-carboxy fluorescein[5] and 1,5-(and-6)-carboxy seminaphthor hodafluor-1-acetoxymethyl ester (SNARF)[6] have been the most widely used fluoroprobes for measuring pHi, primarily because pK_a values are close to physiological pH values of cells and they are available at a relatively low cost. SNARF having excited at one wavelength measures emission at two different wavelengths. For other fluoroprobes, *e.g.*, 2,7-bis-carboxyethyl-5,6-carboxyfluorescein,[7] emission at one wavelength is measured for excitation at two different wavelengths. A rhodamine based fluorescent probes were synthesised and employed to detect fluorescent changes in colorimetric and fluorescent assay.[8–12]

Electron and immune fluorescence microscopy using autophagy related protein (Atg8) as a marker showed that Atg8 is localized to isolation membranes, mature autophagosomes, and autophagic bodies.[4,13] GFP–Atg8 also labels these autophagic structures and further enables the monitoring of autophagy as GFP fluorescence in the vacuolar lumen in living cells.[4,13,14]

The fluoroprobes are usually loaded into cells as an acetoxymethyl ester; this enters the cells readily and is hydrolyzed to yield the free fluorescent dye. The fluorescent ratio can then be determined by one of several methods based on a spectrofluorometer, a fluorescent microscope, or a flow cytometer.[5–7] Fluorescent pH probes usually suffer from optical changes in terms of emission spectra variation and fluorescence intensity,[15] but they have proved effective tools for investigating the role of intracellular pH in diverse physiological and pathological processes, including receptor mediated signal transduction, enzymatic activity, cell growth, apoptosis,[16] ion transport, homeostasis, calcium regulation, endocytosis, chemotaxis, and cell adhesion.[17] They also afford much greater spatial sampling capability and non-invasive measurement, compared with microelectrode techniques.[15,18]

[a]*Polymers and Functional Materials Division, CSIR – Indian Institute of Chemical Technology, Hyderabad-500007, Telangana, India. E-mail: bhosale@iict.res.in; bhosale.iict@gov.in*

[b]*Department of Biotechnology, Deogiri College, Aurangabad-431005, Maharashtra, India. E-mail: krkharat@gmail.com*

[c]*School of Chemical Sciences, Swami Ramanand Teerth Marathwada University, Nanded-431606, Maharashtra, India*

[d]*School of Applied Sciences, RMIT University, GPO Box 2476, Melbourne, VIC-3001, Australia. E-mail: Sheshanath.bhosale@rmit.edu.au*

† Electronic supplementary information (ESI) available: Additional figures, detail experimental protocol, full characterisation and spectroscopic data of all new compounds. See DOI: 10.1039/c5ra24133b

Naphthalenediimide have attracted considerable interest of researchers in material and biological studies due to ease in manipulating their optical and electrochemical properties.[19] We and others have previously employed naphthalenediimides in biological studies.[20] We therefore hypothesized that naphthalenediimide may be used a core moiety for a carboxyl type pH probe for visualizing the cells and autophagosomes that are formed during starvation. More importantly, **NDI-C** was successfully used for the analysis of cell population on the basis of intracellular pH.

The synthetic route of the proposed **NDI-C** compound is shown in Scheme 1. **NDI-C** probes was synthesized by treating tetrabromo naphthalenediimide **1** with 3,4-diaminobenzoic acid at reflux temperature in 66% yield.[21] The solubility of **NDI-C** was limited in comparison to **1**, most probably due to the carboxylic group at the core of **NDI-C**. The ^{1}H NMR of **NDI-C** in DMSO-d_6 showed broad aromatic proton peaks at 6.60 ppm, 7.03 ppm and 7.84 ppm, which was confirmed the core substitution of compound **1** (Scheme 1, Fig. S2†). The aromatic proton peaks of **NDI-C** were gets well resolved after esterification and formation of new –OCH_3 peak at 3.91 ppm in ^{1}H NMR and peaks at 160 ppm and 52.43 ppm in ^{13}C NMR (Scheme S1, Fig. S4, S5 and S13†). The molecular structure of **NDI-C** was consistent with MS and IR characterization (Fig. S1, S3 and S14†).

The synthesized **NDI-C** is non-fluorescent under acidic conditions. Upon the addition of incremental amounts of base the color of fluorophore changed from blue to intense red (Fig. S8†). To get a detailed insight about its optical properties UV-vis and fluorescence experiments were carried out. The UV-vis absorption spectrum of **NDI-C** was measured in Britton–Robinson buffer : DMSO (8 : 2) (Fig. S9a†). **NDI-C** showed visible absorption bands at 294 nm, 418 nm, 440 nm, 575 nm and 625 nm. The change in optical properties of **NDI-C** was further monitored upon changing pH of **NDI-C** solution from 4.53 to 9.89. Upon the addition of base *i.e.* increase in pH of **NDI-C** solution, the absorbance peaks at 294 nm, 418 nm, 440 nm, 575 nm and 625 nm gradually decreased along with color change of solution from blue to intense red (Fig. S9b†). Furthermore, fluorescence emission spectral changes also studied upon addition of base to **NDI-C** (Fig. 1). The excitation (λ_{ex} = 572 nm) of **NDI-C** showed fluorescence emission spectral peaks at 602 and 656 nm. With a change in pH from 4.53 to 9.89, an enhancement in fluorescence emission spectra was observed along with red-shift of the emission band at 602 nm and 656 nm to 615 nm and 665 nm respectively. In addition, the changes in

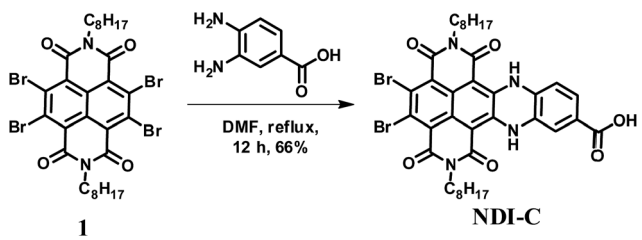

Scheme 1 Synthesis route of NDI-C.

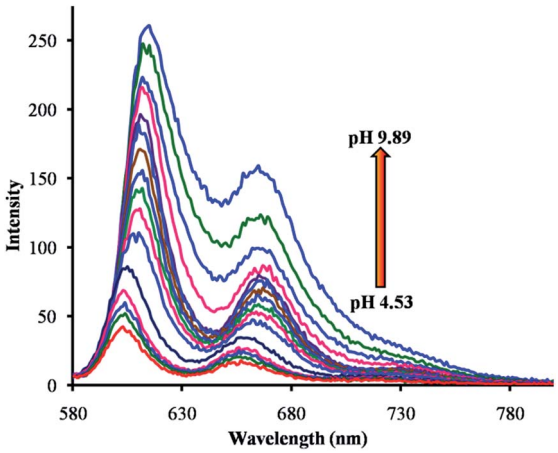

Fig. 1 Fluorescence emission spectra (λ_{ex} = 572 nm) of **NDI-C** (5×10^{-5} M) in Britton–Robinson buffer (buffer/DMSO; 8 : 2) at various pH.

the fluorescence emission intensity of **NDI-C** as a function of pH resulted into a pK_a of 5.59 (Fig. S10†). The obtained fluorescence emission stability properties (Fig. S11†) along with pK_a values clearly indicated that the **NDI-C** could be employed as a sensor for in living cell applications.

The density functional theory (DFT) calculations were carried out using the Gaussian 09 ab initio/DFT quantum chemical simulation package[22] to confirm the electronic distribution on **NDI-C**. The geometry optimization of **NDI-C** (acid and anion) molecules with truncated alkyl chains were carried out at B3LYP/6-311++G** and the polarizable continuum model (PCM) was used to include solvent (DMSO) effect on geometries (Fig. S12†). In order to confirm the obtained geometry of **NDI-C** to be minima on the potential energy surface, frequency calculations were also carried out at the same level of theory, all frequencies were found to be positive. From the obtained molecular geometries, the frontier molecular orbitals of **NDI-C** (acid and anion) were calculated and pictures have been generated by using Avogadro software.[23,24] As shown in Fig. S12† for **NDI-C**, in the ground state the HOMO and LUMO are mainly resides on the NDI core and the carboxylate group. The fluorescence emission intensity increases upon increasing pH. At higher pH, deprotonation of **NDI-C** results into formation of carboxylate ion. In this state electron density are localized on the **NDI-C** moiety as well as carboxylate anion. The **NDI-C** moieties (acid and anion) display a small difference in their band gap (2.42 V and 2.36 V).

The aim of the present investigation on cell line was to analyze the pH of the cells. Skin melanoma cells were used for this analysis. With our aim being to detect the changes in the pH in the cytoplasm, initially, the cells were stained with the **NDI-C** which remained in the cells up to 40 min. The **NDI-C** compound was initially staining the cells a blue color and change in cell pH was observed and indicated by the orange-red areas (Fig. 2A and B).

Furthermore, in search of the autophagosomes in the cells, the cells used were starved for 24 h in phosphate buffer of pH 7.0. The **NDI-C** stains the round bodies in the cell cytoplasm.

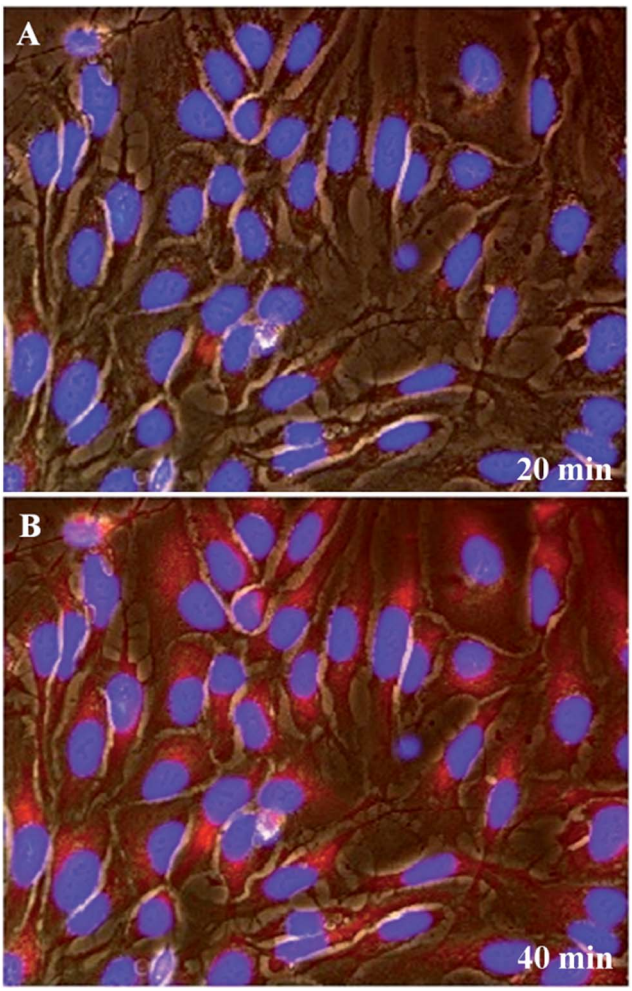

Fig. 2 Fluorescence imaging of NDI-C in skin melanoma cells. NucBlue® Live ReadyProbes® Reagent was added to the wells for the staining of the live cells. The images acquired separately at DAPI light cube, Cy5 light cube and transmitted mode with phase contrast objective. Where (A) after 20 min incubation in a pH 5.2 phosphate buffer; (B) after 40 min incubation in a pH 5.2 phosphate buffer.

The round orange colored autophagosomes were observed in the cells. Due to the acidic pH in the autophagosomes **NDI-C** stains them and cytoplasm show low intensity of the stain in the cells. Nucleus is not stained in the cell with **NDI-C**. The image (Fig. 3) clearly showed the round transparent autophagosomes in cells and the initial stage of **NDI-C** entering in the cells. The autophagosomes detection was monitored for 40 min. These observations indicated that the **NDI-C** was capable of autophagosomes detection. In the control experiment at pH 7, **NDI-C** was added to the SKMEL2 cells to observe the pH changes in the cells. The obtained results showed that the red fluorescence was not detected in the cells (Fig. S15†).

The experiments were also performed to analyze the **NDI-C** pH probe with other fluorescent probes for the detection of the pH in the cell and the autophagosomes. The NucBlue stain was used to locate the nucleus from the cells and the autophagosomes present in the cytoplasm. As the pH decreases in the cytoplasm the **NDI-C** compound will be excreted out slowly

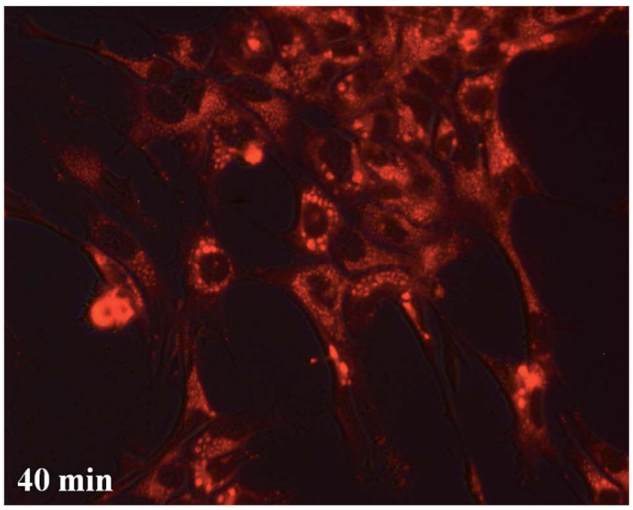

Fig. 3 Fluorescence imaging of NDI-C in skin melanoma cells. The image acquired at Cy5 light cube and transmitted mode with phase contrast objective after 40 min incubation in a pH 5.2 phosphate buffer.

(Fig. 4A). We performed control experiment against starved SKMEL 2. The **NDI-C** was added to SKMEL2 cells along with NucBlue stain. The pH of the cells was 7.2 ± 0.2 (Fig. S16A†). We observed the blue colored nuclei in cells (Fig. S16B and D†). The autophagosomes were not present in the cells and hence not detected after 40 min of incubation at pH 5.2 by fluorescence microscopy (Fig. S16B–D†).

By decreasing the pH the cytoplasm becomes more acidic. After 40 min of incubation the autophagosomes clearly visible as unstained particles in the cell cytoplasm (Fig. 4B). The tracking of the cells after 60 min at pH 4.5 clearly showed that the complete excretion of **NDI-C** and visualization of autophagosomes more precisely (Fig. 4C). The successful full-time tracking of the autophagosomes detection by varying pH indicated the utility of **NDI-C** as a fluorescent marker in cell biology.

To establish the efficiency of **NDI-C** for monitoring the cell population on the basis of intracellular pH, we developed new flow cytometric method. We observed that the **NDI-C** transport is associated with the membrane channels of the cells. The ouabain is a known inhibitor of the Na, K-ATPase used in the experiment. The inhibition of the Na, K-ATPase may lead to changes in the pH of the cells (Warburg effect). The zero h result shows no significant differences in the population (Fig. S17A and C†). A significant change has been observed in the ouabain untreated cells and two distinct populations were observed (Fig. S17B†) whereas only a single population was observed in the ouabain treated cells similar to control (Fig. S17D†). The histogram also shows a distinct population with different pH in ouabain untreated cells (Fig. S18†).

Interestingly, proton pump inhibition results in the acidification of pHi, an event that can be exploited to achieve tumour-specific uptake or activation of certain agents the effect of which are pH-dependent.[25,26] In this context, the capability of our **NDI-C** derivative to sense any drop in the pHi was investigated in

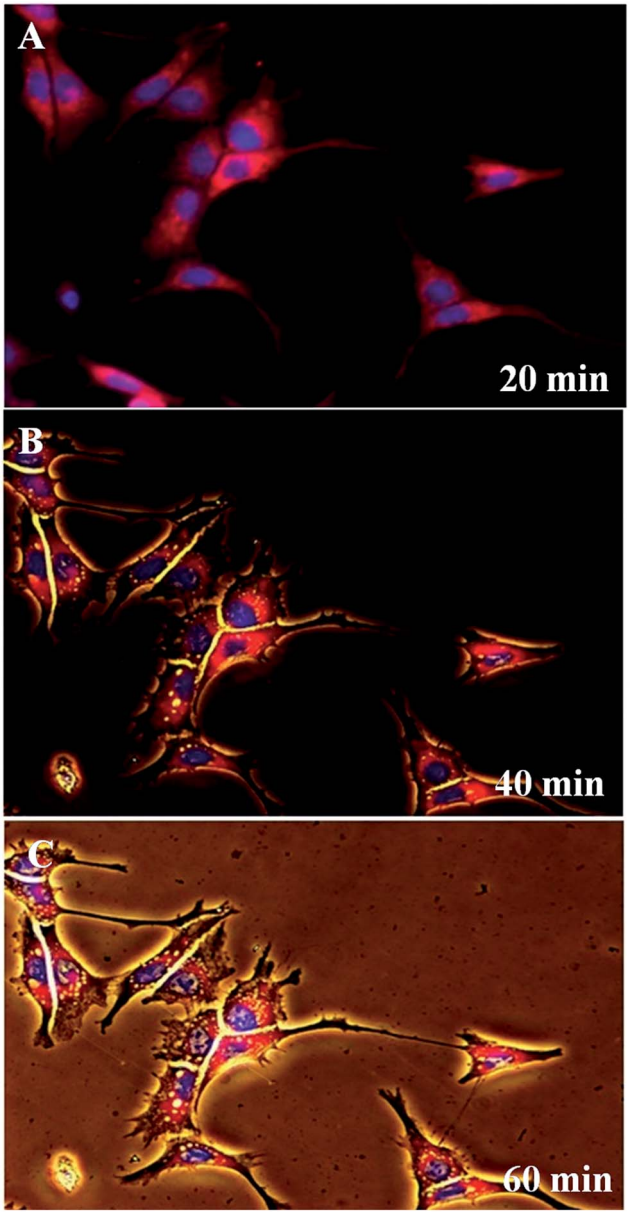

Fig. 4 Fluorescence imaging of **NDI-C** in skin melanoma cells. NucBlue® Live ReadyProbes® Reagent was added to the wells for the staining of the live cells. The images acquired separately at DAPI light cube, Cy5 light cube and transmitted mode with phase contrast objective. Where (A) and (B) after 20 and 40 min incubation in a pH 4.5 phosphate buffer respectively; (C) after 60 min incubation in a pH 4.5 phosphate buffer.

SKMEL2 cells exposed **NDI-C** and subsequently treated with ouabain. Flow cytometric analysis showed that the inhibition of ATPases by ouabain induced an increase in the intensity of the red fluorescence signal originated by **NDI-C**, which concomitantly redistributed within the cytoplasm. Moreover, our findings suggest that **NDI-C** is actually a good pH sensor in cancer cells as the marked increase in the intensity of the fluorescence signal paralleled the Wieder *et al.*,[27] compared the use of two different fluorescent indicators (SNARF and 2,3-dicyanohydroquinone (DCH)) using flow cytometry.

In conclusion, the **NDI-C** used as a new type of probe for analyzing the pH of the cells and autophagosomes formed during starvation. In addition, a new intracellular pH based flow cytometric method optimized for the cells. This probe is unique for the intracellular pH. The Na, K-ATPase pump inhibition study proves the transportation of the pH probe in the cell cytoplasm. The autophagosomes formation in the cells and variation in intracellular pH opened a new way to study the initiation of the starvation in the cancer cells and their possible metastatic potential.

Acknowledgements

S. V. B. (IICT) is grateful for financial support from the DAE-BRNS (Project Code: 37(2)/14/08/2014-BRNS), Mumbai, and Intelcoat project CSC0114, CSIR, New Delhi, India. K. K. would like to thank science and engineering research board SERB, India for the financial support (SR/FT/LS-11/2011). R. S. B acknowledges financial support from CSIR, New Delhi under the SRA scheme [(13(8772)-A)/2015-Pool]. S. V. B. (RMIT) acknowledges financial support from the Australian Research Council under a Future Fellowship Scheme (FT110100152).

Notes and references

1 Z. Xie and D. J. Klionsky, *Nat. Cell Biol.*, 2007, **9**, 1102.
2 T. Noda, K. Suzuki and Y. Ohsumi, *Trends Cell Biol.*, 2002, **12**, 231.
3 S. Elmore, *Toxicol. Pathol.*, 2015, **35.4**, 495.
4 K. Suzuki and Y. Ohsumi, *FEBS Lett.*, 2010, **584**, 1280.
5 C. D. Foster, W. A. G. Hill, T. W. Honeyman and C. R. Scheid, *Am. J. Physiol.*, 1992, **262**, H1651.
6 I. Kurtz and C. Emmons, *Methods Cell Biol.*, 1993, **38**, 183.
7 P. Franck, N. Petitipain, M. Cherlet, M. Dardennes, F. Maachi, B. Schutz, L. Poisson and P. J. Nabet, *BioTechnologia*, 1996, **46**, 187.
8 G. Sivaraman, T. Anand and D. Chellappa, *ChemPlusChem*, 2014, **79**, 1761.
9 H. N. Kim, M. H. Lee, H. J. Kim, J. S. Kim and J. Yoon, *Chem. Soc. Rev.*, 2008, **37**, 1465.
10 X. Chen, T. Pradhan, F. Wang, J. S. Kim and J. Yoon, *Chem. Rev.*, 2012, **112**, 1910.
11 M. Beija, C. S. M. Afonso and J. M. G. Martinho, *Chem. Soc. Rev.*, 2009, **38**, 2410.
12 G. Sivaraman and D. Chellapa, *J. Mater. Chem. B*, 2013, **1**, 57689.
13 T. Kirisako, M. Baba, N. Ishihara, K. Miyazawa, M. Ohsumi, T. Yoshimori, T. Noda and Y. Ohsumi, *J. Cell Biol.*, 1999, **147**, 435.
14 K. Suzuki, T. Kirisako, Y. Kamada, N. Mizushima, T. Noda and Y. Ohsumi, *EMBO J.*, 2001, **20**, 5971.
15 J. B. Pawley, *Handbook of Biological Confocal Microscopy*, Science and Business Media, Springer LLC, New York, USA, 3rd edn, 2006.
16 R. A. Gottlieb and A. Dosanjh, *Proc. Natl. Acad. Sci. U. S. A.*, 1996, **93**, 3587.

17 H. Zhao, X. Xu, J. Diaz and S. Muallem, *J. Biol. Chem.*, 1995, **270**, 19599.
18 M. R. S. Fuh, L. W. Burgess, T. Hirschfeld and G. D. Christian, *Analyst*, 1987, **112**, 1159.
19 S. V. Bhosale, S. V. Bhosale and S. K. Bhargava, *Org. Biomol. Chem.*, 2012, **10**, 6455.
20 S. V. Bhosale, C. H. Jania and S. J. Langford, *Chem. Soc. Rev.*, 2008, **37**, 331.
21 O. Yushchenko, R. V. Hangarge, S. Mosquera-Vazquez, S. V. Bhosale and E. Vauthey, *J. Phys. Chem. B*, 2015, **119**, 7308.
22 M. J. Frisch, *et al.*, *Gaussian 09, Revision.C.01*, Gaussian Inc, Wallingford CT, 2009.
23 Avogadro: an open-source molecular builder and visualization tool. Version 1.1.0, http://www.avogadro.openmolecules.net/.
24 D. Marcus, H. Donald, E. Curtis, D. C. Lonie, T. vandermeersch, E. Zurek and G. R. Hutchison, *J. Cheminf.*, 2012, **4**, 17.
25 K. Zhang, Z. Q. Wang and S. Gluck, *J. Biol. Chem.*, 1992, **267**, 14539.
26 S. Drose and K. Altendorf, *J. Exp. Biol.*, 1997, **200**, 1.
27 E. D. Wieder, H. Hang and M. H. Fox, *Cytometry*, 1993, **14**, 916.

